Modeling and experimental validation of covalent immobilization of *Trametes maxima* laccase on glyoxyl and MANA-Sepharose CL 4B supports, for the use in bioconversion of residual colorants

Bessy V. Cutiño-Avila[1], María I. Sánchez-López[2], Yosberto Cárdenas-Moreno[2], Michael González-Durruthy[3,4], Miguel Ramos-Leal[2,5], Gilda Guerra-Rivera[2], Jorge González-Bacerio[1,6]*, José M. Guisán[7], Juan M. Ruso[4], Alberto del Monte-Martínez[1]*

[1]Centro de Estudio de Proteínas, Facultad de Biología, Universidad de La Habana, La Habana, Cuba

[2]Departamento de Microbiología y Virología, Facultad de Biología, Universidad de La Habana, La Habana, Cuba

[3]LAQV-REQUIMTE of Chemistry and Biochemistry, Faculty of Sciences, University of Porto, Porto, Portugal

[4]Soft Matter and Molecular Biophysics Group, Department of Applied Physics, University of Santiago de Compostela, Santiago de Compostela, Spain

[5]Instituto de Fruticultura Tropical, La Habana, Cuba

[6]Departamento de Bioquímica, Facultad de Biología, Universidad de La Habana, La Habana, Cuba

[7]Departamento de Biocatálisis, Instituto de Catálisis y Petroleoquímica, Consejo Superior de Investigaciones Científicas, Madrid, Spain

Running title: Covalent immobilization of *Trametes maxima* laccase

This article has been accepted for publication and undergone full peer review but has not been through the copyediting, typesetting, pagination and proofreading process, which may lead to differences between this version and the Version of Record. Please cite this article as doi: 10.1002/bab.2125.

ORCIDs and e-mails: bvcutav.88@gmail.com (BVCA); isabel@fbio.uh.cu (MISL); ycardenas@fbio.uh.cu (YCM); gonzalezdurruthy.furg@gmail.com (MGD); fitopatologia18@iift.cu (MRL); ggr@fbio.uh.cu (GGR); 0000-0002-7155-9165, jogoba@fbio.uh.cu (JGB); 0000-0003-1627-6522, jmguisan@icp.csic.es (JMG); juanm.ruso@usc.es (JMR); 0000-0001-9608-5448, adelmonte@fbio.uh.cu (AdMM)

*Corresponding authors: jogoba@fbio.uh.cu (JGB), adelmonte@fbio.uh.cu (AdMM), phone: (53) 7832-4830, fax: (53) 7832-1321

Abstract

Our novel strategy for the rational design of immobilized derivatives (RDID) is directed to predict the behavior of the protein immobilized derivative before its synthesis, by the usage of mathematic algorithms and bioinformatics tools. However, this approach needs to be validated for each target enzyme. The objective of this work was to validate the RDID strategy for covalent immobilization of the enzyme laccase from *Trametes maxima* MUCL 44155 on glyoxyl- and monoaminoethyl-N-aminoethyl (MANA)-Sepharose CL 4B supports. Protein surface clusters, more probable configurations of the protein-supports systems at immobilization pHs, immobilized enzyme activity and protein load were predicted by $RDID_{1.0}$ software. Afterward, immobilization was performed and predictions were experimentally confirmed. As a result, the laccase-MANA-Sepharose CL 4B immobilized derivative is better than laccase-glyoxyl-Sepharose CL 4B in predicted immobilized derivative activity (63.6 % *vs*. 29.5 %). Activity prediction was confirmed by an experimental expressed enzymatic activity of 68 %, using 2,6-dimethoxyphenol as substrate. Experimental maximum protein load match the estimated value (11.2 ± 1.3 *vs.* 12.1 protein mg / support mL). The laccase-MANA-Sepharose CL 4B biocatalyst has a high specificity for the acid blue 62 colorant. The results obtained in this work suggest the possibility of using this biocatalyst for wastewater treatment.

Keywords: colorant bioconversion; covalent immobilization; immobilized derivative activity; laccase; rational design of immobilized derivatives strategy

Abbreviations: 2,6-DMP, 2,6-dimethoxyphenol; %Dec, Decolorization percentage; %FC, percentage of functional competence; %FCP, percentage of functional competence in all population; AB 62, acid blue 62; AB 113, acid blue 113; AB 116, acid blue 116; ABTS, 2,2'-azinobis-3-ethylbenzothiazoline-6-sulfonic acid; BiocatDecAct, biocatalyst decolorizing activity; N-term, amino terminal group; cCP, covalent configuration probability; C-term, carboxyl terminal group; DA, deviation angle; diff. IG (prot), differential protein immobilization grade; eMQ, estimated maximum quantity of protein to immobilize; FEB, Gibbs free energy of binding; ImmDer. FC, immobilized derivative functional competence; MANA, monoaminoethyl-N-aminoethyl; mMQ, molar maximum quantity of protein to immobilize; OEC, operational effectiveness coefficient; PDB, protein data bank; pMQ, practical maximum quantity of protein to immobilize; RDID, rational design of immobilized derivatives; RMSD, root-mean-square deviation; tMA, theoretical maximum activity; tMQ, theoretical maximum quantity of protein to immobilize; tRA, theoretical residual activity; U, unit of enzymatic activity; v_{reac}, reaction rate

1. Introduction

Protein immobilization is probably the most used technology to increase the operational stability of these molecules, achieved via multipoint covalent attachment, multisubunit immobilization (for multimeric proteins) or generation of favorable environments. An appropriate immobilization may also improve enzyme activity, selectivity or specificity, may reduce inhibition or be coupled to enzyme purification (1-4). Therefore, immobilization has enhanced protein usage in the synthesis of

affinity matrices, biocatalysts for enzymatic bioconversion processes and other analytical and biomedical applications (5-11).

Since the 90s decade it has occurred an important transition in the development of immobilized derivatives (12). Very few works have been focused on the rational design of immobilized derivatives. They are mainly about the rational design of biocatalysts (13). The term "rational design" has been used to indicate the optimization of the main parameters in the immobilization process, such as the immobilization conditions (time, pH, additives, ionic strength and load) and the support properties (form, pore diameter, particle size) (12,14-16). Other approximations are based on protein engineering, as directed evolution and site-specific mutagenesis (2-4,17-19).

Due to the high cost of proteins and supports, and the requirements to increase the efficiency of immobilized systems, it is necessary to rationalize and optimize the processes of obtainment of immobilized derivatives, on the basis of their physical-chemical characteristics and applications. Today, the design of immobilized systems is very complex and it is usually empirically performed (experimental screening or protein engineering). The empirical optimization requires many experiments, and the discrimination among the different variables that are affecting the system is hard.

The strategy for the rational design of immobilized derivatives (RDID) works in a different way. This can be defined as the previous process in the searching for a solution for the synthesis of immobilized derivatives. Rational design is directed to predict the behavior of the immobilized derivative before its synthesis, by the usage of mathematic algorithms and bioinformatics tools. In this manner, it is possible to select the optimum conditions for its synthesis. Rational design complements the experimental screening (20-25).

The industrial development in the last decades has implicated the release of high amounts of highly toxic residual chemical compounds and high volumes of residual waters, which exhibit a high content

of colorants (26). Among the most used enzymes for dye decolorization and bioremediation are oxidoreductases, such as peroxidases, azoreductases and laccases (27-29). The microorganisms traditionally used to remove the colorants in textile wastes are the basidiomycete white-rot fungi (30,31). The fungal species from the *Trametes* genus produce the ligninolytic enzyme, high redox potential laccase, in high concentrations. This monomeric enzyme oxidizes phenols and polyphenols, the components of lignin. In addition, laccase is able to catalyze the oxidation of different aromatic recalcitrant compounds. Therefore, it is used to remove colorants (32,33).

For this reason, the objective of this work was to validate our RDID strategy for covalent immobilization of the enzyme laccase from *Trametes maxima* MUCL 44155 on glyoxyl- and monoaminoethyl-N-aminoethyl (MANA)-Sepharose CL 4B supports (very known and used porous solid supports), for the use of the resultant biocatalysts in bioconversion of residual colorants present in textile industry wastes. The following immobilization parameters were calculated: most probable configuration and functional competence of the immobilized derivatives, and maximum quantity of protein to immobilize. All developed mathematic algorithms were automatized in the $RDID_{1.0}$ software (Python language). The laccase enzyme was immobilized on both supports, according to the immobilization parameters predicted by the $RDID_{1.0}$ software. Last, a molecular docking was performed to study the interaction between laccase and some residual colorants, and the activity of the best immobilized derivative on bioconversion of some of these colorants was evaluated.

2. Materials and Methods

2.1. Computational methodology

The experimentally obtained laccase 3D structure was obtained from the protein data base RCSB Protein Data Bank (http://www.rcsb.org/pdb; PDB code: 2H5U (34)). Structural analyses were

performed using the molecular visor PyMol (35). The deviation angle (*DA*) parameter was calculated using the plug-in eMovie from the PyMol software.

The software *RDID*$_{1.0}$© (Enzyme Technology Group (20)) was used to predict the possible clusters in the laccase surface and to calculate the parameter covalent configuration probability (*cCP*) for each cluster. This software was also used to calculate the *DA*, the percentage of functional competence (*%FC*; catalytic competence in the particular case of enzymes), the percentage of functional competence in all population (*%FCP*), the immobilized derivative functional competence (*ImmDer. FC*), the theoretical maximum activity (*tMA*) and the theoretical residual activity (*tRA*). *DA* is the angle between the active site entrance of the immobilized enzyme and the normal straight line to the support. *%FC* is the percentage of functionally (catalytically) competent enzymes, regarding all the molecules immobilized through the same cluster of reactive groups. It is calculated according to: *%FC* = 100 % - *DA* × 1.11 % (the functional competence of the cluster is penaltied in 1.11 % for each deviation angle degree). *%FCP* is the percentage of functionally competent enzymes in each cluster, regarding the whole immobilized derivative. It is calculated according to: *%FCP* = *cCP* × *%FC*. *ImmDer. FC* is the percentage of functionally competent enzymes in the whole immobilized derivative (adding up the *%FCP* of all clusters). It is calculated according to: *ImmDer. FC* = Σ*%FCP*. *tMA* is the theoretical maximum activity that can be immobilized, assuming that all immobilized enzymes are functionally competent. It is calculated according to: *tMA* = soluble specific enzymatic activity × estimated maximum quantity of protein to immobilize (*eMQ*). On the other hand, *tRA* is the theoretical residual activity that can be immobilized, considering the immobilized derivative functional competence. It is calculated according to: *tRA* = *tMA* × *ImmDer. FC* / 100 (21,22).

In addition, the *RDID*$_{1.0}$ software was used to calculate the parameters: molar maximum quantity of protein to immobilize (*mMQ*), theoretical maximum quantity of protein to immobilize (*tMQ*),

operational effectiveness coefficient (*OEC*), and *eMQ*, which are additional components of the RDID strategy (21).

2.2. Protein immobilization

Covalent immobilization of laccase enzyme from *T. maxima* MUCL 44155 (homogeneously purified enzyme was obtained in the Microbial Biotechnology Group, Faculty of Biology, University of Havana) was performed on glyoxyl- and MANA-Sepharose CL 4B supports. Glyoxyl-Sepharose CL 4B support (contains aldehyde groups for protein immobilization) was prepared using the method described by Guisán (36), and MANA-Sepharose CL 4B support (shows amino groups for protein immobilization) was obtained by the procedure reported by Fernández-Lafuente *et al*. (37). Both supports were highly-activated supports (36,37).

With the first support, immobilization was performed with 1 mL glyoxyl-Sepharose CL 4B support plus 9 mL of protein solution (in the range: 0.11-5.56 mg/mL or 1-50 protein mg / support mL) in 0.1 M sodium phosphate buffer pH 7.0, according to Guisán (36). The mixture was shaken all night at 20ºC. Immobilization on MANA-Sepharose CL 4B support was performed at pH 5.0 according to Fernández-Lafuente *et al*. (37) using the same protein load range. For each immobilization method, non-activated Sepharose CL 4B support was used as a control.

Immobilization was controlled by the parameter differential protein immobilization grade (*diff. IG (prot)*) (38). The experimental parameter practical maximum quantity of protein to immobilize (*pMQ*) was calculated from the obtained *diff. IG (prot)* values (21). Protein concentration was assessed by the Bradford method (39) in 96-well plates. Bovine serum albumin was used as standard protein. All assays were performed by triplicate. Immobilized enzymatic activity was determined by the differential method (soluble initial activity - activity in filtrates and washes after immobilization), and it is expressed in units of enzymatic activity per support mL. Expressed enzymatic activity was

determined by the same differential method, but it is expressed in percentage taking as 100 % the soluble initial enzymatic activity.

2.3. Assessment of laccase enzymatic activity

Laccase activity was assessed monitoring the absorbance at 469 nm, related with the oxidation of 140 mM 2,6-dimethoxyphenol (2,6-DMP) in 0.1 M sodium acetate buffer pH 5.0. The 2,6-DMP molar extinction coefficient is 27.5 M^{-1} cm^{-1} (40). Reactions were performed in 1 mL cuvettes at 25ºC with 0.05 mL of protein sample. The experiments were performed by triplicate. One unit (U) of enzymatic activity was defined as the enzyme amount able to oxidize 1 μmol 2,6-DMP per min under the assay conditions.

2.4. Molecular docking simulations

To evaluate the interaction between laccase from *Trametes maxima* and reference ligands 2,2'-azinobis-3-ethylbenzothiazoline-6-sulfonic acid (ABTS; non-phenolic substrate) and 2,6-DMP, as well as recalcitrant colorants acid blue 62 (AB 62; molecular mass 422.4 g/mol; C.I. number 62045; molecular formula $C_{20}H_{19}N_2NaO_5S$), acid blue 113 (AB 113; molecular mass 681.7 g/mol; C.I. number 26360; molecular formula $C_{32}H_{21}N_5Na_2O_6S_2$) and acid blue 116 (AB 116; molecular mass 681.7 g/mol; C.I. number 26380; molecular formula $C_{32}H_{21}N_5Na_2O_6S_2$), molecular docking simulations were performed according to Cárdenas-Moreno *et al*. (41).

2.5 Decolorization studies with colorants present in textile wastes and the immobilized derivative laccase-MANA-Sepharose CL 4B

For bioconversion studies, the colorants AB 62, AB 113 and AB 116 were used, gently donated by Yorkshire Group (Tertre, Belgium). The reaction mixture contained 0.1 M sodium acetate buffer pH 3.5, and reactions were performed at 30ºC and 100 rpm for 24 h in thermostatic shaker (Infors AG, Switzerland). In these experiments, the immobilized biocatalyst of laccase from *T. maxima* was

synthesized at its *pMQ* (11.2 protein mg / support mL for MANA-Sepharose CL 4B). Masic concentration of colorants was 70 mg/L. However, molar concentration was 208 μmol/mL for AB 62 and 109 μmol/mL for AB 113 and AB 116. Two controls were used: non-activated Sepharose CL 4B and MANA-Sepharose CL 4B supports with the aim to discard the colorant unspecific adsorption to support and assess the colorant stability in bioconversion conditions (42). The experiments were performed by triplicate.

Decolorization percentage (%Dec) was spectrophotometrically assessed using the optical density at the λ of maximum absorption of each colorant (AB 62, 595 nm; AB 116, 565 nm; AB 113, 600 nm). The equation is the following: $\%Dec = (OD_i - OD_f) / OD_i \times 100$; where: OD_i and OD_f are initial and final optical densities, respectively. The reaction rate (v_{reac}) was calculated according to the following equation: $v_{reac} = ((\%Dec / 100) \times ([colorant] \times V_T) / (t \times V_B)) \times dilution$; where: V_T is the total assay volume (1 mL), t is the total assay time (1440 min), and V_B is the volume of immobilized biocatalyst used in the assay (5 μL). In addition, the biocatalyst decolorizing activity (BiocatDecAct), expressed in μmol / min / biocatalyst g, was determined.

3. Results

3.1. Prediction of the most probable configurations of laccase from *Trametes maxima* on glyoxyl- and MANA-Sepharose CL 4B supports

Firstly, the possible clusters to immobilize laccase on glyoxyl- (pH 7.0) and MANA-Sepharose CL 4B (pH 5.0) supports, and their respective *cCP* values (21), were predicted by *RDID*$_{1.0}$ software (Table 1; Fig. 1). Clusters 1 were the most probable for both immobilizations (*cCP* of 0.98 for glyoxyl- and 0.37 for MANA-Sepharose CL 4B), since both contain the higher number of reactive residues (Table 1).

3.2. Prediction of the functional competence of the immobilized derivatives laccase-glyoxyl- and laccase-MANA-Sepharose CL 4B

Predictions of *%FC*, *%FCP* and *ImmDer. FC* parameters for the covalent immobilization of laccase on glyoxyl-Sepharose CL 4B, indicate that only enzymes immobilized through cluster 1 are active, due to the combination of an elevated *cCP* (0.98; Table 1) and a favorable *DA* (63º; Fig. 1 top; Table 2). This immobilized derivative has only 29.5 % of immobilized molecules with activity (Table 2). In contrast, covalent immobilization of laccase on MANA-Sepharose CL 4B support has a significant contribution of the enzyme immobilized by the four first clusters, due to their *cCP* values (0.37, 0.23, 0.17 and 0.15, respectively; Table 1) and a high active sites exposure (*DA* = 2º, 40º, 35º and 65º, respectively; Fig. 1 bottom; Table 2). An *ImmDer. FC* of 63.6 % was predicted for this immobilized derivative.

3.3. Prediction of theoretical parameters *mMQ*, *tMQ* and *eMQ* for covalent immobilization of laccase from *Trametes maxima* on glyoxyl- and MANA-Sepharose CL 4B supports

Predicted *mMQ*, *tMQ* and *eMQ* values were 0.81 μmol, 43.2 mg and 12.1 mg of laccase per support mL, respectively (Table 3). In addition, *OEC* was 0.28.

3.4. Immobilization of *Trametes maxima* laccase enzyme on glyoxyl- and MANA-Sepharose CL 4B supports

The experimental results derived of the immobilization of *T. maxima* laccase on glyoxyl- and MANA-Sepharose CL 4B supports were compared with the predictions corresponding to the *in silico* optimization of the immobilization. As is shown in Table 3, experimentally obtained *pMQ* values were lower than the predicted *tMQ* one, but equal to *eMQ* value. In the same manner, immobilized and expressed enzymatic activity, experimentally determined, are equal or very similar to predicted *tRA* and *ImmDer. FC*, respectively, for each immobilized derivative (Table 3).

3.5. Prediction of *Trametes maxima* laccase-colorant interaction by molecular docking

Before testing different model colorants from the textile industry wastes in bioconversion ability of the immobilized derivatives, the interaction between laccase and these molecules was predicted by molecular docking. First, the binding active-site was predicted (Fig. 2). This binding active-site is composed by neutral and acid residues, as well as cystein.

Second, the flexibility of the laccase molecule was evaluated (Fig. 3). This enzyme shows a central core with low flexibility, composed mainly by β sheets, and highly-flexible peripheric regions conformed by β sheets, loops and one α-helix.

Third, hydrophobic interactions (the main) between laccase and the model colorants were evaluated by molecular docking (Table 4). Two additional reference controls, ABTS and 2,6-DMP, were tested. The highest affinity was predicted for the AB 62 colorant, with a Gibbs free energy of binding (FEB) of -8.6 kcal/mol. In contrast, the lowest affinity was registered for the ligand 2,6-DMP, with a FEB of -5.2 kcal/mol. The *RMSD* of the complexes were in the range 0.145-2.145 Å (Table 4).

In Fig. 4 are shown the aminoacid residues of laccase enzyme involved in interactions with colorants or ligands. The residues that establish interactions in at least four complexes were L^{112}, S^{113}, P^{346}, E^{460} and Y^{491}. It is notable that the complex with the lowest affinity, laccase-2,6-DMP (Table 4), is stabilized by the lowest number of interactions, only eight (Fig. 4).

3.6. Bioconversion of model colorants by the immobilized biocatalyst *Trametes maxima* laccase-MANA-Sepharose CL 4B

For bioconversion assays, the laccase-MANA-Sepharose CL 4B biocatalyst was selected, due to its higher immobilized and expressed enzymatic activity (70 U / support mL and 68 %, respectively; Table 3). In addition, the colorants AB 62, AB 113 and AB 116 were selected (Fig. 5), including the compound with the highest affinity for laccase enzyme (AB 62; Table 4).

Unspecific adsorption of colorants to the support was studied, using two controls: non-activated Sepharose CL 4B and MANA-Sepharose CL 4B. Coherently with the bioconversion assays, this study was performed for five bioconversion cycles. The behavior of colorant unspecific adsorption was similar in the two controls (Fig. S1). After first cycle, more than 40 % of colorants were adsorbed to the supports (41.9, 44.9 and 48.5 % for AB 62, AB 113 and AB 116, respectively). In the second cycle, the percentages of unspecific adsorption decreased, being 1.3, 2.1 and 3.2 % for AB 62, AB 113 and AB 116, respectively. From the third cycle the supports, once saturated, did not adsorb more colorants.

The operational stability of the immobilized derivative in bioconversion assays was high, due to %Dec were maintained above 91 % in five bioconversion cycles (Table 5). Only for AB 116 colorant, %Dec was fewer than 70 % from the fourth cycle, probably produced by the enzyme inactivation.

Other bioconversion parameters, for reactions performed at 30ºC and pH 3.5 for 24 h, are shown in Table 5. The activity of immobilized biocatalyst toward AB 62 colorant resulted in $v_{reac} > 54 \times 10^{-3}$ μmol/mL/min, as well as BiocatDecAct > 76 μmol/min/biocatalyst g, in five bioconversion cycles. For the others two colorants, the values of these parameters were approximately the half.

4. Discussion

In this work, the RDID strategy was successfully used to model the covalent immobilization of *T. maxima* laccase enzyme on glyoxyl- and MANA-Sepharose CL 4B supports. The *RDID*$_{1.0}$ software allowed predicting the system behavior and the optimal conditions of the immobilization process before to synthesize the immobilized derivatives. These predictions were confirmed by experimental results.

Clusters are zones in the protein surface that contain residues with potentialities for immobilization (residues with amino groups for glyoxyl- and carboxyl groups for MANA-Sepharose). Laccase from *T. maxima* has very few lysines on the surface (Fig. 1 top). For this reason, there are very few enzyme-support binding sites for immobilization on glyoxyl-Sepharose CL 4B support. The *pKa* values of lysine epsilon amino groups are high (around 10.5), and probabilities that they are not protonated at pH 7.0 are low. Therefore, the amino terminal is the only reactive group at this pH. This implies a low probability to obtain multipunctual enzyme-support covalent bonds, and endangers the operational stability of the immobilized derivative.

It has been reported that, at pH 7.0, the probability to immobilize a monomeric protein in highly activated supports with glyoxyl groups is very low, because the only reactive amino group at this pH is the amino terminal, and a single amino-glyoxyl bond is not stable enough for immobilization (1,43). However, we performed laccase immobilization on glyoxyl-Sepharose support over-night (the maximal time assayed in the cited works was 7 h at neutral pH) at 20ºC (the temperature at which the highest relative immobilization rate was obtained in those works). We used this long time for immobilization due to laccase enzyme was homogeneous, and the absence of contaminant proteases ensures enzyme stability. During this time, increases the probability to obtain more enzyme molecules bound to the support by Schiff's bases (ready for the reduction step to obtain irreversible secondary amino bonds) and single-point immobilized enzyme, or even a very low proportion of multipoint immobilized molecules involving some lysine epsilon amino groups. To work at pHs higher than 7.0, would considerably increase the reactivity of lysine epsilon amino groups and the probabilities to obtain multipunctual bonds. However, previous studies demonstrated some enzyme inactivation when immobilization was performed at these pHs (Microbial Biotechnology Group, Faculty of Biology, University of Havana (unpublished data)).

Acid residues are abundant at the protein surface, conforming six clusters (Table 1; Fig. 1 bottom). Reactivities of aspartic and glutamic acids are high at pH 5.0, due to they have too low *pKa* values, generally lower than 4.0. Consequently, MANA-Sepharose CL 4B support (activated with primary amino groups with low *pKa* values (37)) shows high probabilities for the obtainment of multibound immobilized derivatives, operationally more stables.

Due to the low *ImmDer. FC* predicted for the laccase-glyoxyl-Sepharose CL 4B immobilized derivative (29.5 %; Table 2), aldehyde-activated supports are not recommended for immobilization of laccase enzyme from *T. maxima*. However, the MANA-Sepharose CL 4B support is better than the previous support for the immobilization of this enzyme, since an *ImmDer. FC* of 63.6 % was predicted for the resultant immobilized derivative (Table 2).

$RDID_{1.0}$ software allowed predicting the parameters *mMQ*, *tMQ* and *eMQ* for covalent immobilization of laccase from *Trametes maxima* on glyoxyl- and MANA-Sepharose CL 4B supports (Table 3). *tMQ* is calculated considering ideal conditions for immobilization. To calculate *tMQ*, only the support total area and the protein diameter are considered. Other variables that can affect the protein amount to immobilize, such as diffusional restrictions, are not considered (21). For *tMQ* calculations, we assumed that: (i) the protein ligand is a sphere, and its projection on the support surface is a circle; (ii) the support surface is totally covered by a monolayer of protein molecules; and (iii) diffusional restrictions can be ignored, only valid when the support pore diameter is much higher than the protein size. This maximum theoretical value is only reached for very small proteins. In this work, *tMQ* is higher than the predicted *eMQ* value (Table 3).

On the contrary, the *eMQ* is the maximum quantity of protein that can be theoretically immobilized, taking into account diffusional restrictions. It is a correction of the *tMQ* which considers these diffusional restrictions through the *OEC* parameter. *eMQ* is the product between *tMQ* and *OEC* (20). Therefore, *eMQ* is closer to the experimental values (21). The parameter *OEC* (0.28 in this work;

Table 3) considers the relationship between the protein diameter and the support pore diameter, and allows estimating the extension in that the diffusional restrictions can affect the protein amount to immobilize (21). *T. maxima* laccase is not a small protein (diameter = 65.6 Å), compared with the support pore diameter (1023 Å). This causes that the optimal relationship protein diameter : support pore diameter (1:20 or 0.05) is not fulfilled (the actual ratio is higher: 1:15.6 or 0.06). For this reason, this system is diffusionally restricted ($OEC < 0.45$), explaining the differences between *tMQ* and *eMQ* (43.2 *vs*. 12.1 protein mg / support mL; Table 3) (21).

The similarity between *pMQ* and *eMQ* (11.2 ± 1.3 *vs*. 12.1 protein mg / support mL; Table 3) demonstrates the reliability of $RDID_{1.0}$ predictions. This result indicates that optimal initial protein load for immobilization can be predicted without performing an experimental loading study. This avoids discarding time and reagents. In the case of perform experimental loading study, *eMQ* is equally useful, since it provides information about the protein load range that should be assayed (around *eMQ*). On the other hand, results derived from the comparison between experimental data and predicted values for the functional activity of the immobilized derivatives (Table 3), support the use of RDID strategy to optimize covalent immobilization of laccase enzyme, in function of the functional competence of resultant biocatalysts. Experimental results confirm that MANA-Sepharose CL 4B support is the best, between both assayed supports, for immobilization of *T. maxima* laccase, with an expressed enzymatic activity of 68 % (Table 3).

Enzyme immobilization on solid supports is essential for the development of industrial processes based on biotransformations catalyzed by these enzymes. Immobilization allows enzyme recovery and reutilization in discontinuous reactors, since the protein can be separated from the other components of the reaction mixture. In this sense, this also favors the product purity. On the other hand, the development of continuous processes of enzyme-catalyzed reactions only makes sense if the enzyme is immobilized inside the reactor.

Previous studies support the effectiveness of molecular docking to predict the laccase ability for dye decolorization (44-46). In this work, the docking results suggest, and bioconversion assays confirm, that the three tested colorants are substrates of *T. maxima* laccase. In a previous work, using the laccase from the fungus *Ganoderma weberianum* and five ligands of potential biotechnological interest (three antibiotics and two xenobiotics), the enzyme-ligand interactions were modeled by molecular docking and identified a high prevalence of hydrophobic interactions with laccase binding residues (41). These authors predicted a lower affinity of laccase enzyme for these ligands, in comparison with the present work, as show higher FEB values (from -6.8 to -4.7 kcal/mol). However, the FEB for the two controls, ABTS and 2,6-DMP (-7.1 and -4.8 kcal/mol, respectively), were very similar to those obtained in this work (-7.9 and -5.2 kcal/mol, respectively; Table 4).

Our predictions about *T. maxima* laccase residues involved in interactions with ligands (Fig. 4) require experimental confirmation. Currently, the effective interactions between substrates and laccase active site are under discussion. Some authors attribute to the substrate redox potential a more important role in reactivity than interactions with enzyme active site (47). When different binding modes were predicted, a relevant role of D^{206} and H^{458} (*T. versicolor* and *T. maxima* laccase numbering) for substrate recognition was identified (48). These results differ from our data for the only common compound between both studies (2,6-DMP). These differences could be attributed to the use of different enzymes (*T. versicolor* laccase in the reference work) and docking softwares (Glide in the reference study, AutoDock Vina in this work). However, five enzyme residues (L^{112}, S^{113}, P^{346}, E^{460} and Y^{491}) interacting with at least four ligands, among two controls and three colorants, were predicted in our study (Fig. 4). This supports the quality of our docking methodology and results.

Docking was performed considering the soluble enzyme, and not taking into account its expected orientation on the immobilization support (Fig. 1). However, since we predicted the most probable

configurations of the laccase-support systems (Fig. 1), and we also predicted the functional competence of these configurations (based on active site accessibility for substrates) (Table 2), we indirectly consider the possibility to establish productive enzyme-colorant interactions. These interactions were experimentally confirmed by bioconversion assays (Table 5), discarding the adoption of inactive conformations by the immobilized enzyme.

Bioconversion results show a higher operational stability of the immobilized derivative on AB 113 colorant bioconversion, compared with AB 116 (Table 5), in spite of structural difference between both colorants is only the position of sulphonic substituent (Fig. 5). On the other hand, immobilized laccase has a higher specificity for the AB 62 colorant, as show the bioconversion parameters (Table 5). This higher specificity is consistent with the higher affinity predicted for laccase-AB 62 complex (Table 4).

The obtained %Dec for the three colorants are comparable, and in many cases higher than, the reported ones for other immobilized derivatives of laccase enzyme. Wang *et al*. (49), using an initial concentration of the colorant Red B-3BF of 50 mg/mL only obtained a 50 % decolorization after 10 cycles. Zhang *et al*. (50), after six cycles, demonstrated that *Coriolus versicolor* laccase maintains the 50 % of decolorizing activity. Similarly, Kunamneni *et al*. (51), after five cycles, retained the 41 % of activity in decolorization of methyl green dye with a laccase immobilized on supports activated with epoxy groups. The results obtained in this work show %Dec that suggest the possibility of using this biocatalyst on a large scale.

5. Authors' contribution

BVCA: Investigation. MISL: Conceptualization, Data curation, Formal analysis, Investigation, Methodology. YCM: Investigation. MGD: Conceptualization, Data curation, Formal analysis,

Funding acquisition, Methodology, Resources. MRL: Methodology, Supervision. GGR: Methodology, Supervision. JGB: Conceptualization, Formal analysis, Methodology, Writing - original draft, Writing - review & editing. JMG: Funding acquisition, Resources, Supervision. JMR: Funding acquisition, Resources, Supervision. AdMM: Conceptualization, Data curation, Formal analysis, Methodology, Project administration, Software, Supervision, Roles/Writing - original draft, Writing - review & editing. All authors read and approved the manuscript.

6. Conflicts of interest/Competing interests

The authors declare that they have no conflict of interests or competing interests.

7. Funding

This research did not receive any specific grant from funding agencies in the public, commercial, or not-for-profit sectors.

8. References

1. Mateo, C., Abian, O., Bernedo, M., Cuenca, E., Fuentes, M., Fernández-Lorente, G., Palomo, J.M., Grazu, V., Pessela, B.C.C., Giacomini, C., Irazoqui, G., Villarino, A., Ovsejevi, K., Batista-Viera, F., Fernández-Lafuente, R., Guisán, J.M. (2005) *Enz. Microbiol. Technol*. **37**, 456-462.

2. Hernández, K., Fernández-Lafuente, R. (2011) *Enz. Microbiol. Technol*. **48**, 107-122.

3. Bernal, C., Rodríguez, K., Martínez, R. (2018) *Biotechnol. Adv*. **36**, 1470-1480.

4. Bilal, M., Iqbal, H.M.N., Guo, S., Hu, H., Wang, W., Zhang, X. (2018) *Int. J. Biol. Macromol*. **108**, 893-901.

5. Boudrant, J., Cheftel, C. (1976) *Biotechnol. Bioeng*. **18**, 1735-1749.

6. Chen, S.T., Hsiao, S.C., Chiou, A.J., Wu, S.H., Wang, K.T. (1992) *J. Chin. Chem. Soc*. **39**, 91-99.

7. Palomo, J.M., Fernández-Lorente, G., Mateo, C., Fuentes, M., Fernández-Lafuente, R., Guisán, J.M. (2002) *Tetrahedron: Asymm.* **13**, 1337-1345.

8. Palomo, J.M., Fernández-Lorente, G., Mateo, C., Fernández-Lafuente, R., Guisán, J.M. (2002) *Tetrahedron: Asymm*. **13**, 2375-2381.

9. Palomo, J.M., Filice, M., Fernández-Lafuente, R., Terreni, M., Guisán, J.M. (2007) *Adv. Synth. Cat*. **349**, 1969-1976.

10. Palomo, J.M. (2009) *Curr. Org. Synth*. **6**, 1-14.

11. Mateo, C., Palomo, J.M., Fernández-Lorente, G., Fernández-Lafuente, R., Guisán, J.M. (2007) *Enz. Microbiol. Technol*. **40**, 1451-1463.

12. Cao, L. (2005) Carrier-bound immobilised enzymes: Principles, application and design, Wiley-VCH, Weinheim.

13. Bornscheuer, U.T., Pohl, M. (2001) *Curr. Opin. Chem. Biol*. **5**, 137-143.

14. van Roon, J.L., Schroën, C.G.P.H., Tramper, J., Beeftink, H.H. (2007) *Biotechnol. Adv*. **25**, 137-147.

15. Vermue, M.H., Tramper, J. (1995) *Pure Appl. Chem*. **67**, 345-373.

16. Dib, I., Nidetzky, B. (2008) *BMC Biotechnol*. **8**, 72-83.

17. Turkova, J. (1999) *J. Chrom. B* **722**, 11-31.

18. Cecchini, D.A., Serra, I., Ubiali, D., Terreni, M., Albertini, A.M. (2007) *BMC Biotech*. **7**, 54-65.

19. Serra, I., Cecchini, D.A., Ubiali, D., Manazza, E.M., Albertini, A.M., Terreni, M. (2009) *Eur. J. Org. Chem*. 1384-1389.

20. del Monte, A., Cutiño, B., Gil, D., Mokarzel, L., González, J., Pupo, M., Chávez, M.Á., Pons, T., Díaz, J. (2010) *Serie Cient. Univ. Cienc. Inf. (Cuba)* **3**(3), 185-202.

21. del Monte-Martínez, A., Cutiño-Avila, B.V., González-Bacerio, J., in Sandoval, G., Ed. (2018) Lipases and phospholipases: Methods and protocols, Meth. Mol. Biol., vol. 1835, Springer Science+Business Media, LLC, pp. 243-283.

22. del Monte-Martínez, A., Cutiño-Avila, B., González-Bacerio, J., Chávez, M.Á., Díaz, J., Guisán, J.M., in Chávez, M.Á., Díaz, J., Arias, O., Eds. (2019) Nano-micro-biotecnologías y sus aplicaciones, Editorial UH, Havana, pp. 155-180.

23. Torres-Salas, P., del Monte-Martínez, A., Cutiño-Avila, B., Rodríguez-Colina, B., Alcalde, M., Ballesteros, A.O., Plou, F.J. (2011) *Adv. Mater*. **23**, 5275-5282.

24. del Monte, A., Cutiño, B., Gómez, D., Pereda, I., Díaz, J., Rojas, J. (2013) *IFMBE Proceeds* **33**, 73-76.

25. del Monte-Martínez, A., Cutiño-Avila, B., González-Bacerio, J., Chávez, M.Á., Díaz, J. (2014) *Anal. Acad. Cien. Cuba* **4**, 1-15.

26. Mishra, A., Kumar, F. (2009) *J. Biochem. Eng*. **46**, 251-256.

27. Routoula, E., Patwardhan, S.V. (2020) *Environ. Sci. Technol.* **54**, 647-664.

28. Bao, J., Catucci, G., Valetti, F. (2020) *Biotechnol. Appl. Biochem.* **Editorial**, 711-713. DOI: 10.1002/bab.2046.

29. Catucci, G., Valetti, F., Sadeghi, S.J., Gilardi, G. (2020) *Biotechnol. Appl. Biochem.* 1-9. DOI: 10.1002/bab.2015.

30. Enayatzamir, K., Hossein, A.A., Yakhchali, B., Tabandeh, F., Rodríguez-Couto, S. (2010) *Environ. Sci. Pollut. Res*. **17**, 145-153.

31. Vaithanomsat, P., Apiwatanapiwat, W., Petchoy, O., Chedchant, J. (2010) *Int. J. Chem. Eng*. DOI: 10.1155/2010/162504.

32. Diorio, L.A., Mercuri, A.A., Nahabedian, D.E., Forchiassin, F. (2008) *Chemosphere* **72**, 150-156.

33. Raghukumar, C., D'Souza-Ticlo, D., Kumar, A. (2008) *Crit. Rev. Microbiol*. **34**, 189-206.

34. Lyashenko, A.V., Zhukhlistova, N.E., Gabdoulkhakov, A.G., Zhukova, Y.N., Voelter, W., Zaitsev, V.N., Bento, I., Stepanova, E.V., Kachalova, G.S., Koroleva, O.V., Cherkashyn, E.A., Tishkov, V.I., Lamzin, V.S., Schirwitz, K., Morgunova, E. Y., Betzel, C., Lindley, P.F., Mikhailov, A.M. (2006) *Acta Crystallogr. Sect. F* **62**, 954-957.

35. DeLano, W.L. (2002) The PyMOL molecular graphics system, DeLano Scientific, San Carlos.

36. Guisán, J.M. (1988) *Enz. Microbiol. Technol*. **10**, 375-382.

37. Fernández-Lafuente, R., Rosell, C.M., Rodríguez, V., Santana, C., Soler, G., Bastida, A., Guisán, J.M. (1993) *Enz. Microbiol. Technol*. **15**, 546-550.

38. del Monte-Martínez, A., González-Bacerio, J., Aragón-Abreu, C., Palomo-Carmona, J.M., Guisán-Seijas, J.M., Díaz-Brito, J. (2012) *Rev. CENIC Cienc. Biol*. **43**, 3-8.

39. Bradford, M.M. (1976) *Anal. Biochem*. **72**, 248-254.

40. Zouari-Mechichi, H., Mechichi, T., Dhouib, A., Sayadi, S., Martínez, A.T., Martínez, M.J. (2006) *Enz. Microbiol. Technol*. **39**, 141-148.

41. Cárdenas-Moreno, Y., Espinosa, L.A., Vieyto, J.C., González-Durruthy, M., del Monte-Martinez, A., Guerra-Rivera, G., Sánchez-López, M.I. (2019) *Ann. Proteom. Bioinform*. **3**, 001-009. DOI: 10.29328/journal.apb.1001007.

42. Osma, J.F., Herrera, J.L.T., Rodríguez-Couto, S. (2010) *App. Catal. A* **373**, 147-153.

43. Fernández-Lorente, G., López-Gallego, F., Bolívar, J.M., Rocha-Martín, J., Moreno-Perez, S., Guisán J.M. (2015) *Curr. Org. Chem*. **19**, 1-13.

44. Prasad, N.K., Vindal, V., Narayana, S.L., Ramakrishna, V., Kunal, S.P., Srinivas, M. (2012) *J. Mol. Model*. **18**, 2013-2019.

45. Sridhar, S., Chinnathambi, V., Arumugam, P., Suresh, P.K. (2013) *Appl. Biochem. Biotechnol*. **169**, 911-922.

46. Singh, D., Kant Sharma, K., Jacob, S., Gakhar, S.K. (2014) *Water Air Soil Pollut*. **225**, 2175. DOI: 10.1007/s11270-014-2175-7.

47. Beck, S., Berry, E., Duke, S., Milliken, A., Patterson, H., Prewett, D.L., Carter Rae,. T., Sridhar, V., Wendland, N., Gregory, B.W., Johnson, C.M. (2018) *Int. Biodet. Biodeg.* **127**, 146-159.

48. Mehra, R., Muschiol, J., Meyer, A.S., Kepp, K.P. (2018) *Sci. Rep.* **8**, 17285. DOI: 10.1038/s41598-018-35633-8.

49. Wang, P., Fan, X., Cui, L., Wang, Q., Zhou, A. (2008) *J. Environ. Sci*. **20**, 1519-1522.

50. Zhang, J., Xua, Z., Chena, H., Zong, Y. (2009) *Biochem. Eng. J*. **45**, 54-59.

51. Kunamneni, A., Ghazia, I., Camarero, S., Ballesteros, A., Plou, F.J., Alcalde, M. (2008) *Process Biochem*. **43**, 169-178.

Tables

Table 1 $RDID_{1.0}$ predictions of the possible clusters and covalent configuration probabilities for immobilization of *Trametes maxima* laccase enzyme on glyoxyl- and MANA-Sepharose CL 4B supports

Immobilized derivative (-Sepharose CL 4B support)	**Cluster number**	**Protein residues**	***cCP***

laccase-glyoxyl-; pH 7.0	1	N-term, K^{192}, K^{194}	0.98
	2	K^{324}, K^{475}	0.01
	3	K^{59}	0.01
laccase-MANA-; pH 5.0	1	D^{7}, D^{42}, D^{96}, D^{128}, D^{138}, D^{142}, D^{143}, D^{282}	0.37
	2	C-term, D^{364}, D^{486}, D^{492}	0.23
	3	D^{323}, D^{364}, D^{470}, D^{473}	0.17
	4	D^{234}, D^{255}, E^{288}	0.15
	5	D^{435}	0.04
	6	D^{180}	0.05

cCP: covalent configuration probability. N-term: amino terminal group. C-term: carboxyl terminal group

Table 2 $RDID_{1.0}$ predictions for the functional competence of the *Trametes maxima* laccase enzyme covalently immobilized on glyoxyl- and MANA-Sepharose CL 4B supports

Immobilized derivative (-Sepharose CL 4B support)	**Cluster number**	***DA***	***%FC* (%)**	***%FCP* (%)**	***ImmDer. FC* (%)**
laccase-glyoxyl-; pH 7.0	1	63º	30.1	29.5	29.5

	2	126º	0.0	0.0	
	3	114º	0.0	0.0	
laccase-MANA-; pH 5.0	1	2º	97.8	36.2	63.6
	2	40º	55.6	12.8	
	3	35º	61.2	10.4	
	4	65º	27.9	4.2	
	5	180º	0.0	0.0	
	6	128º	0.0	0.0	

DA: deviation angle. *%FC*: percentage of functional competence. *%FCP*: percentage of functional competence in all population. *ImmDer. FC*: immobilized derivative functional competence

Table 3 Experimental values of protein load and enzymatic activity in the immobilized derivatives laccase-glyoxyl- and laccase-MANA-Sepharose CL 4B, and comparison with the values predicted by the $RDID_{1.0}$ software

mMQ **(protein µmol / support mL)**	***tMQ*** **(protein mg / support mL)**	***OEC***	***eMQ*** **(protein mg / support mL)**	**Immobilized derivative (-Sepharose CL 4B support)**	***pMQ*** **(protein mg / support mL)**	**Initial enzymatic activity (U/mL)**	**Immobilized enzymatic activity (U / support mL)**	***tRA*** **(U / support mL)**	**Expressed enzymatic activity (%)**	***ImmDer. FC*** **(%)**
0.81	43.2	0.28	12.1	laccase-glyoxyl-	11.7 ± 1.2	103.1 ±	36.1 ± 4.1	32.0 ± 2.4	35 ± 3.6	29.5

				pH 7.0		9.8				
				laccase-MANA- pH 5.0	11.2 ± 1.3		70.1 ± 6.5	69.0 ± 5.6	68 ± 5.6	63.6

mMQ: molar maximum quantity of protein to immobilize. *tMQ*: theoretical maximum quantity of protein to immobilize. *OEC*: operational effectiveness coefficient. *eMQ*: estimated maximum quantity of protein to immobilize. *pMQ*: practical maximum quantity of protein to immobilize. *tRA*: theoretical residual activity. *ImmDer. FC*: immobilized derivative functional competence. Data are presented as means ± standard deviations

Table 4 Specific hydrophobic interactions of the best docking complexes laccase-ligand

Ligands	**Docking complexes**	**Docking affinity** **(FEB: kcal/mol)**	***RMSD* (Å)**
ABTS	laccase-ABTS	-7.9	0.145
2,6-DMP	laccase-2,6-DMP	-5.2	0.246
AB 62	laccase-AB 62	-8.6	1.791
AB 116	laccase-AB 116	-7.5	2.145
AB 113	laccase-AB 113	-7.5	1.576

ABTS: 2,2'-azinobis-3-ethylbenzothiazoline-6-sulfonic acid. 2,6-DMP: 2,6-dimethoxyphenol. AB 62: acid blue 62. AB 116: acid blue 116. AB 113: acid blue 113. FEB: Gibbs free energy of binding. *RMSD*: root-mean-square deviation

Table 5 Bioconversion parameters of the laccase-MANA-Sepharose CL 4B biocatalyst for colorants present in textile industry wastes

Colorant	**Bioconversion cycle**	**v_{reac} (10^{-3} μmol/mL/min)**	**%Dec**	**BiocatDecAct (μmol / min / biocatalyst g)**
AB 62	1	55.9 ± 5.4	96.9 ± 9.5	78.3 ± 7.6
	2	54.4 ± 6.1	94.2 ± 9.3	76.2 ± 7.8
	3	55.5 ± 4.9	96.1 ± 8.8	77.8 ± 7.5
	4	54.3 ± 5.4	94.1 ± 9.5	76.1 ± 7.6
	5	54.8 ± 4.5	95.0 ± 9.6	76.8 ± 7.4
AB 113	1	29.6 ± 3.1	98.0 ± 9.7	41.6 ± 4.3
	2	29.4 ± 2.8	97.2 ± 9.7	41.2 ± 4.0
	3	29.2 ± 3.1	97.0 ± 9.5	41.0 ± 4.5
	4	29.1 ± 2.7	96.2 ± 9.6	40.8 ± 4.2
	5	28.3 ± 2.9	93.8 ± 9.5	26.7 ± 2.8
AB 116	1	28.4 ± 2.6	93.7 ± 9.1	39.7 ± 4.2
	2	28.1 ± 2.9	92.7 ± 8.9	39.3 ± 3.9
	3	27.5 ± 2.8	91.0 ± 9.1	38.6 ± 3.5

	4	19.8 ± 2.1	65.6 ± 7.0	27.8 ± 2.8
	5	19.0 ± 1.8	62.9 ± 5.9	26.7 ± 2.5

AB 62: acid blue 62. AB 113: acid blue 113. AB 116: acid blue 116. v_{reac}: Reaction rate. %Dec: Decolorization percentage. BiocatDecAct: biocatalyst (laccase-MANA-Sepharose CL 4B) decolorizing activity. Each bioconversion cycle was for 24 h

Figure legends

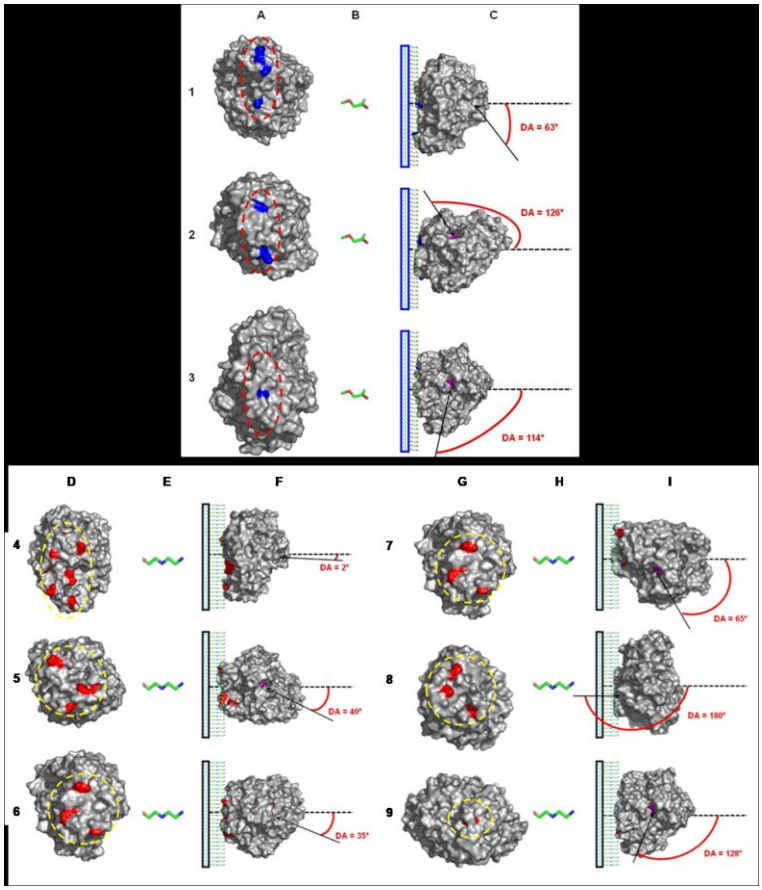

FIG 1 Graphical representation of the different possible configurations of *Trametes maxima* laccase-glyoxyl- and laccase-MANA-Sepharose CL 4B supports systems, predicted by *RDID*$_{1.0}$ software from

the predicted clusters at pH 7.0 and 5.0, respectively. (1-3) Clusters 1-3 for laccase-glyoxyl-Sepharose CL 4B. (4-9) Clusters 1-6 for laccase-MANA-Sepharose CL 4B. (A, D and G) Possible clusters in laccase (surface representation) for covalent immobilization on glyoxyl-Sepharose CL 4B support at pH 7.0 (A) and MANA-Sepharose CL 4B support at pH 5.0 (D and G). (B, E and H) Support functional groups (glyoxyl for B and monoaminoethyl-N-aminoethyl for E and H). (C, F and I) Most probable configuration of the immobilized derivatives by each cluster. *DA*: deviation angle. Grey: enzyme surface area. Blue and red: residues with amino (blue) and carboxyl (red) groups on the enzyme surface. Pink: active site (signaled by an arrow). Dotted red and yellow circles: cluster delimitation. For interpretation of the references to color in this figure legend, the reader is referred to the Web version of this article.

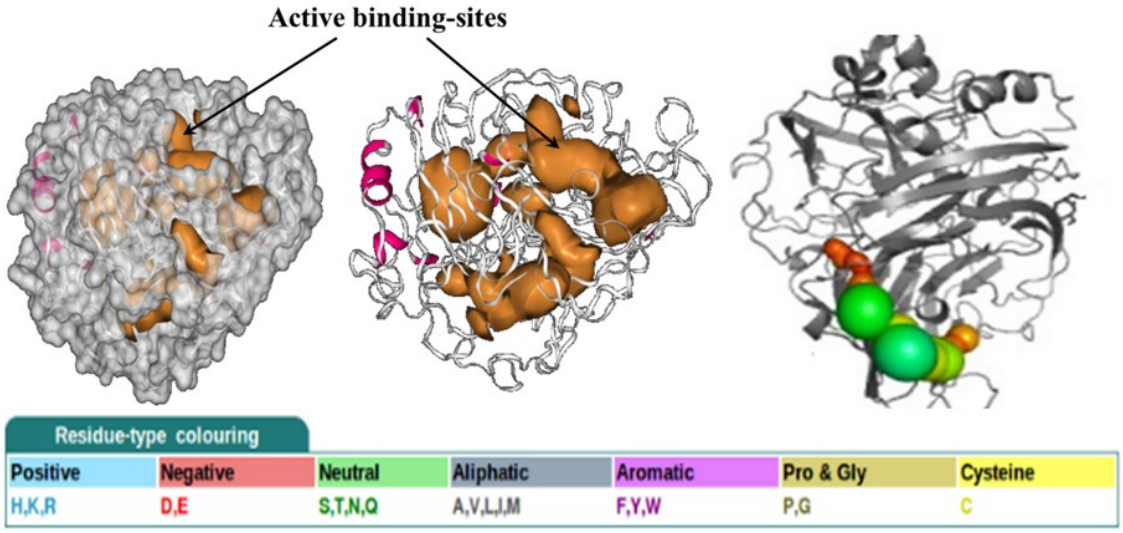

FIG 2 Binding active-site prediction for *T. maxima* laccase. Left: DeepSite prediction of topological cavities of laccase (PDB code: 2H5U) binding active-site (volumetric orange regions). Right: Physical-chemical properties of aminoacid residues in the binding active-site of laccase. For interpretation of the references to color in this figure legend, the reader is referred to the Web version of this article.

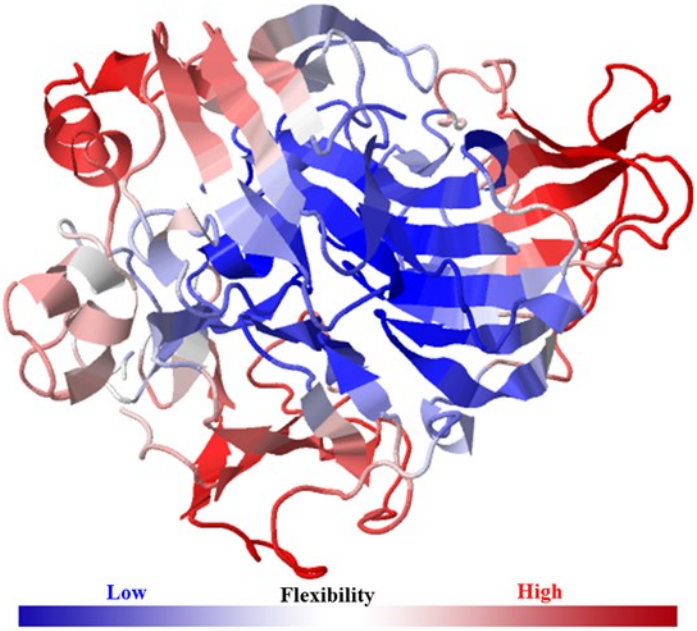

FIG 3 *T. maxima* laccase flexibility properties. Low flexibility (blue) and high flexibility regions (red) are represented. For interpretation of the references to color in this figure legend, the reader is referred to the Web version of this article.

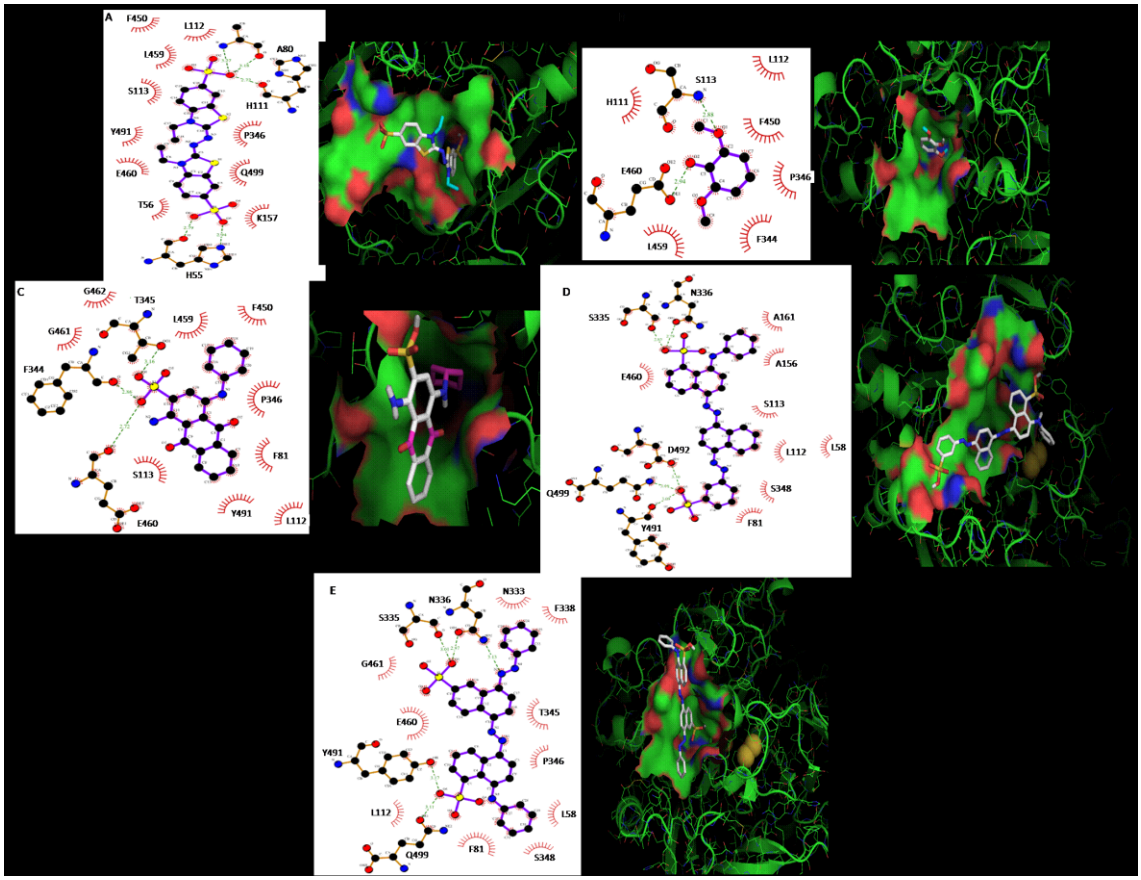

FIG 4 Modeled laccase-ligand complexes. 2D Lig-Plot diagrams and van der Waals surface of laccase active-site representation for the (A) ABTS-, (B) 2,6-DMP-, (C) AB 62-, (D) AB 113- and (E) AB 116-laccase interactions. Hydrogen bonds are represented by discontinuous lines. Ligands are represented as sticks and balls (2D Lig-Plot) and sticks (in van der Waals surface representation). Colors: black or grey for ligands and green for residues, oxygen red, nitrogen blue and sulfur yellow. For interpretation of the references to color in this figure legend, the reader is referred to the Web version of this article.

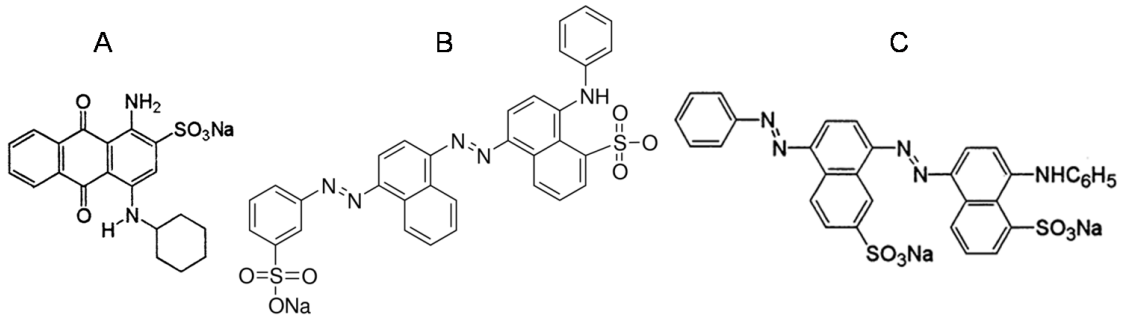

FIG 5 Structures of colorants used in the bioconversion experiments. (A) AB 62. (B) AB 113. (C) AB 116.